A novel GABA-mediated corticotropin-releasing hormone secretory mechanism in the median eminence

NEUROSCIENCE

10.1126/sciadv.1501723

A novel GABA-mediated corticotropin-releasing hormone secretory mechanism in the median eminence

Keisuke Kakizawa,[1,2] Miho Watanabe,[1] Hiroki Mutoh,[1] Yuta Okawa,[1,2] Miho Yamashita,[2] Yuchio Yanagawa,[3] Keiichi Itoi,[4] Takafumi Suda,[2] Yutaka Oki,[5] Atsuo Fukuda[1]*

Corticotropin-releasing hormone (CRH), which is synthesized in the paraventricular nucleus (PVN) of the hypothalamus, plays an important role in the endocrine stress response. The excitability of CRH neurons is regulated by γ-aminobutyric acid (GABA)–containing neurons projecting to the PVN. We investigated the role of GABA in the regulation of CRH release. The release of CRH was impaired, accumulating in the cell bodies of CRH neurons in heterozygous GAD67-GFP (green fluorescent protein) knock-in mice (GAD67$^{+/GFP}$), which exhibited decreased GABA content. The $GABA_A$ receptor ($GABA_AR$) and the Na^+-K^+-$2Cl^-$ cotransporter (NKCC1), but not the K^+-Cl^- cotransporter (KCC2), were expressed in the terminals of the CRH neurons at the median eminence (ME). In contrast, CRH neuronal somata were enriched with KCC2 but not with NKCC1. Thus, intracellular Cl^- concentrations ($[Cl^-]_i$) may be increased at the terminals of CRH neurons compared with concentrations in the cell body. Moreover, GABAergic terminals projecting from the arcuate nucleus were present in close proximity to CRH-positive nerve terminals. Furthermore, a $GABA_AR$ agonist increased the intracellular calcium (Ca^{2+}) levels in the CRH neuron terminals but decreased the Ca^{2+} levels in their somata. In addition, the increases in Ca^{2+} concentrations were prevented by an NKCC1 inhibitor. We propose a novel mechanism by which the excitatory action of GABA maintains a steady-state CRH release from axon terminals in the ME.

INTRODUCTION

The hypothalamic-pituitary-adrenal (HPA) axis is activated by a variety of stressors, and corticotropin-releasing hormone (CRH) plays a key role in HPA axis regulation. The cell bodies of CRH neurons are present in the paraventricular nucleus (PVN) of the hypothalamus, from which their axons pass through the lateral retrochiasmatic area and project to the median eminence (ME) (*1*). CRH released from the external layer of the ME (*2*) activates the secretion of adrenocorticotropic hormone (ACTH) from the anterior pituitary, which subsequently activates the synthesis and secretion of glucocorticoids from the adrenal glands.

The activities of CRH neurons in the PVN are regulated by various neurotransmitters, including norepinephrine, glutamate, and γ-aminobutyric acid (GABA) [for a review, see the study of Levy and Tasker (*3*)]. GABA is synthesized from glutamate by the two isoforms of glutamate decarboxylase (GAD), GAD65 and GAD67 (*4*). Under nonstressful conditions, GABAergic inputs, which originate from the anterior perifornical region, the anterior hypothalamic area ventral to the PVN, the perinuclear zone of the supraoptic nucleus, the rostral region of the PVN itself, and the bed nucleus of the stria terminals (*5*–*9*), exert an inhibitory action on CRH neurons in the PVN (*3*, *5*, *6*). This GABAergic inhibition requires relatively low intracellular Cl^- concentrations ($[Cl^-]_i$), which are maintained by the K^+-Cl^- cotransporter (KCC2) in mature neurons (*10*). In contrast, if an animal is exposed to an acute stressor, then GABA excites the CRH neurons as a result of an increase in $[Cl^-]_i$ caused by KCC2 internalization (*11*, *12*). Moreover, decreased GABAergic inhibitory regulation of CRH neurons, which is induced by the same mechanism involved in the response to acute stress, has been proposed as one of the mechanisms that induce depression-like behavior during chronic stress (*13*). We previously reported that basal plasma corticosterone levels are significantly lower in heterozygous GAD67-GFP (green fluorescent protein) knock-in mice (GAD67$^{+/GFP}$ mice), which exhibit reduced GABA synthesis (*14*), than they are in wild-type mice (*15*). On the basis of these findings under nonstressful conditions, a mechanism different from the one responsible for the inhibition of CRH neurons at the level of the somata is hypothesized to be responsible for the effects of GABA on the HPA axis.

It has been reported that GABA (*16*) and $GABA_A$ receptors ($GABA_ARs$) (*17*) are present in the region of the ME where the CRH neurons terminate in the capillary walls. However, it is not yet known whether GABA controls CRH release at the ME, which may play a pivotal role in the HPA axis. Here, we investigate the mechanism by which GABAergic inputs control CRH release from axon terminals at the level of the ME.

[1]Department of Neurophysiology, Hamamatsu University School of Medicine, Hamamatsu, Shizuoka 431-3192, Japan. [2]Second Division, Department of Medicine, Hamamatsu University School of Medicine, Hamamatsu, Shizuoka 431-3192, Japan. [3]Department of Genetic and Behavioral Neuroscience, Gunma University Graduate School of Medicine, Maebashi, Gunma 371-8511, Japan. [4]Laboratory of Information Biology, Graduate School of Information Sciences, Tohoku University, Sendai, Miyagi 980-8579, Japan. [5]Department of Family and Community Medicine, Hamamatsu University School of Medicine, Hamamatsu, Shizuoka 431-3192, Japan.
*Corresponding author: Email: axfukuda@hama-med.ac.jp

RESULTS

Alterations in the functions of CRH neurons via reduced GAD67-mediated GABA synthesis

We previously reported that basal plasma corticosterone levels are significantly decreased in GAD67$^{+/GFP}$ mice compared with levels in

wild-type mice (*15*); however, the statuses of the other HPA axis parameters in GAD67$^{+/GFP}$ mice are not yet known. The basal plasma corticosterone and ACTH levels at 0900 to 1200 in the GAD67$^{+/GFP}$ mice were significantly decreased compared with the levels in the wild-type mice regardless of sex [females: corticosterone—wild type, 92.7 ± 7.4 ng/ml; GAD67$^{+/GFP}$, 65.1 ± 9.9 ng/ml; ACTH—wild type, 93.3 ± 5.2 pg/ml; GAD67$^{+/GFP}$, 79.0 ± 2.9 pg/ml; males: corticosterone—wild type, 63.3 ± 5.0 ng/ml; GAD67$^{+/GFP}$, 42.1 ± 8.1 ng/ml; ACTH—wild type, 83.6 ± 4.1 pg/ml; GAD67$^{+/GFP}$, 65.0 ± 5.1 pg/ml; only data from males are shown in the graphs; n = 5 to 6 mice per experimental group; $P < 0.05$, Student's t test; Fig. 1, A and B]. Therefore, we used only males for subsequent experiments. In contrast, there were no significant differences in the plasma corticosterone and ACTH levels at 1900 to 2000 (corticosterone: wild type, 79.1 ± 4.78 ng/ml; GAD67$^{+/GFP}$, 61.4 ± 10.0 ng/ml; ACTH: wild type, 154.6 ± 18.1 pg/ml; GAD67$^{+/GFP}$, 144.9 ± 25.9 pg/ml; n = 6 to 8 mice per experimental group; Fig. 1, A and B). Therefore, we examined only samples collected from mice at 0900 to 1200 for subsequent experiments. The basal plasma levels of arginine vasopressin (AVP), which activates ACTH secretion from the anterior pituitary (*18*), were also not significantly different between genotypes (wild type, 3.5 ± 1.0 pg/ml; GAD67$^{+/GFP}$, 4.8 ± 3.3 pg/ml; n = 5 mice per experimental group; Fig. 1C). We also examined plasma corticosterone and ACTH levels in response to a single 30-min bout of restraint-induced stress, and there was no significant difference between genotypes (corticosterone: wild type, 133.0 ± 9.3 ng/ml; GAD67$^{+/GFP}$, 162.4 ± 10.8 ng/ml; ACTH: wild type, 862.0 ± 150.9 pg/ml; GAD67$^{+/GFP}$, 776.1 ± 181.7 pg/ml; n = 5 to 6 mice per experimental group; Fig. 1, A and B). To determine whether the function of the CRH neurons was also altered in the GAD67$^{+/GFP}$ mice under nonstressful conditions at 0900 to 1200, we performed immunohistochemistry for CRH in the PVN (Fig. 2, A to C) using the anti-CRH primary antibody, the specificity of which was verified in a CRH-iCre mouse line (fig. S1, A to C). The density and intensity of the CRH-immunoreactive cells in the PVN were significantly increased in GAD67$^{+/GFP}$ mice compared with wild-type mice (density: wild type, 3700 ± 248.3/mm^2; GAD67$^{+/GFP}$, 4766.7 ± 120.2/mm^2; intensity: wild type, 2.35 ± 0.08; GAD67$^{+/GFP}$, 3.01 ± 0.27), whereas the mean areas of the CRH-immunoreactive cells were not significantly different between the two groups (wild type, 56.7 ± 5.3 μm^2; GAD67$^{+/GFP}$, 66.1 ± 2.2 μm^2; $P < 0.05$, Student's t test; Fig. 2D). The CRH mRNA expression levels in the hypothalamus were equivalent in both genotypes (n = 6 mice per experimental group; Fig. 2E). The CRH content in the PVN, measured via radioimmunoassay (RIA), was significantly increased in GAD67$^{+/GFP}$ mice compared with wild-type mice (wild type, 3.5 ± 0.4 μg per mouse; GAD67$^{+/GFP}$, 4.4 ± 0.2 μg per mouse). However, there was no significant difference in CRH content in the ME (wild type, 2.0 ± 0.3 μg per mouse; GAD67$^{+/GFP}$, 1.9 ± 0.2 μg per mouse; n = 10 mice per experimental group; $P < 0.05$, Student's t test; Fig. 2F). These findings suggest that the CRH peptide may accumulate in the cell bodies of CRH neurons in the PVN of GAD67$^{+/GFP}$ mice as a result of reduced CRH release in the ME. The decreased plasma corticosterone and ACTH levels in the GAD67$^{+/GFP}$ mice may also be explained by this hypothesis.

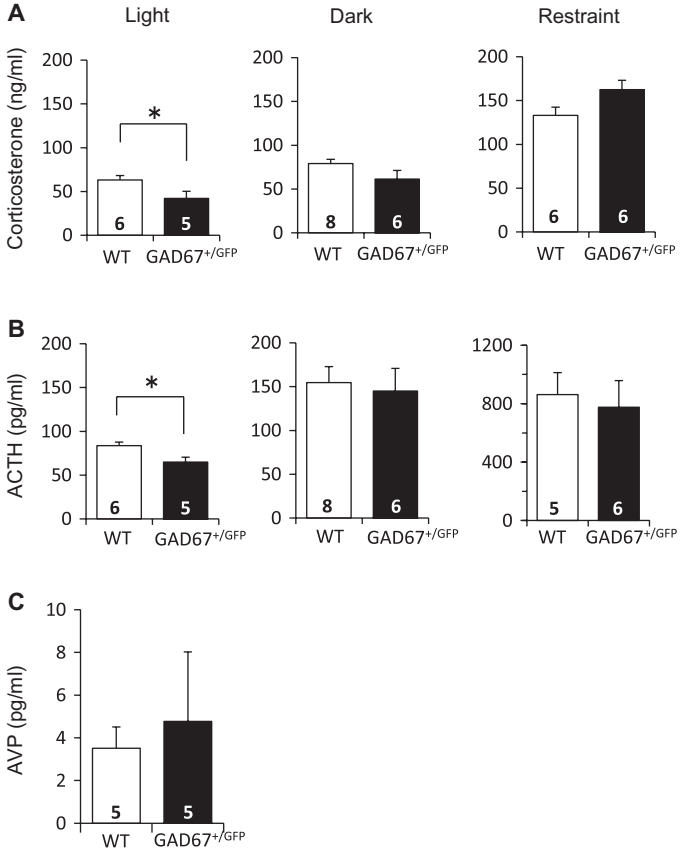

Fig. 1. Reduced GAD67-mediated GABA synthesis affected basal HPA axis parameters. (**A** and **B**) The plasma corticosterone and ACTH levels in the adult male wild-type (WT) and GAD67$^{+/GFP}$ mice at 0900 to 1200 (light), 1900 to 2000 (dark), and after a single 30-min bout of restraint-induced stress. Both the corticosterone and ACTH levels at 0900 to 1200 were significantly decreased in the GAD67$^{+/GFP}$ mice. (**C**) The basal plasma AVP levels in the male mice were not different between the two groups. *$P < 0.05$; Student's t tests. Error bars represent SEM. The sample sizes are indicated within the bars.

Axonal transport–dependent accumulation of somatic CRH

To investigate whether the neuronal accumulation of CRH in the GAD67$^{+/GFP}$ mice is altered under stressful conditions, we performed CRH immunohistochemistry on the PVN after a single 30-min bout of restraint-induced stress (Fig. 2, G and H). The density of the CRH-immunoreactive cells in the PVN increased after a bout of restraint-induced stress to the point that it was equivalent between the genotypes. The fluorescence intensity and mean area of the CRH-immunoreactive cells were also not significantly different between the genotypes after the induction of stress (density: wild type, 4438 ± 366.4/mm^2; GAD67$^{+/GFP}$, 5316.7 ± 235.1/mm^2; intensity: wild type, 2.40 ± 0.16; GAD67$^{+/GFP}$, 2.54 ± 0.08; area: wild type, 60.3 ± 4.7 μm^2; GAD67$^{+/GFP}$, 59.2 ± 3.9 μm^2; Fig. 2I). On the basis of these results, we hypothesized that the difference in CRH immunoreactivity between wild-type and GAD67$^{+/GFP}$ mice is masked when CRH neurons are activated. To test this hypothesis, we performed CRH immunohistochemistry on the PVN of adult mice that had undergone bilateral adrenalectomy (ADX) to reduce the feedback inhibition on the CRH neurons and increase CRH production (Fig. 3, A to D). The density of the detectable CRH-immunoreactive cells and the fluorescence intensity of these CRH neurons in the PVN of the wild-type mice increased after ADX, and they were comparable with that of the GAD67$^{+/GFP}$ mice (density: wild type, 4533.3 ± 405.5/mm^2; GAD67$^{+/GFP}$, 4700 ± 208.2/mm^2; intensity:

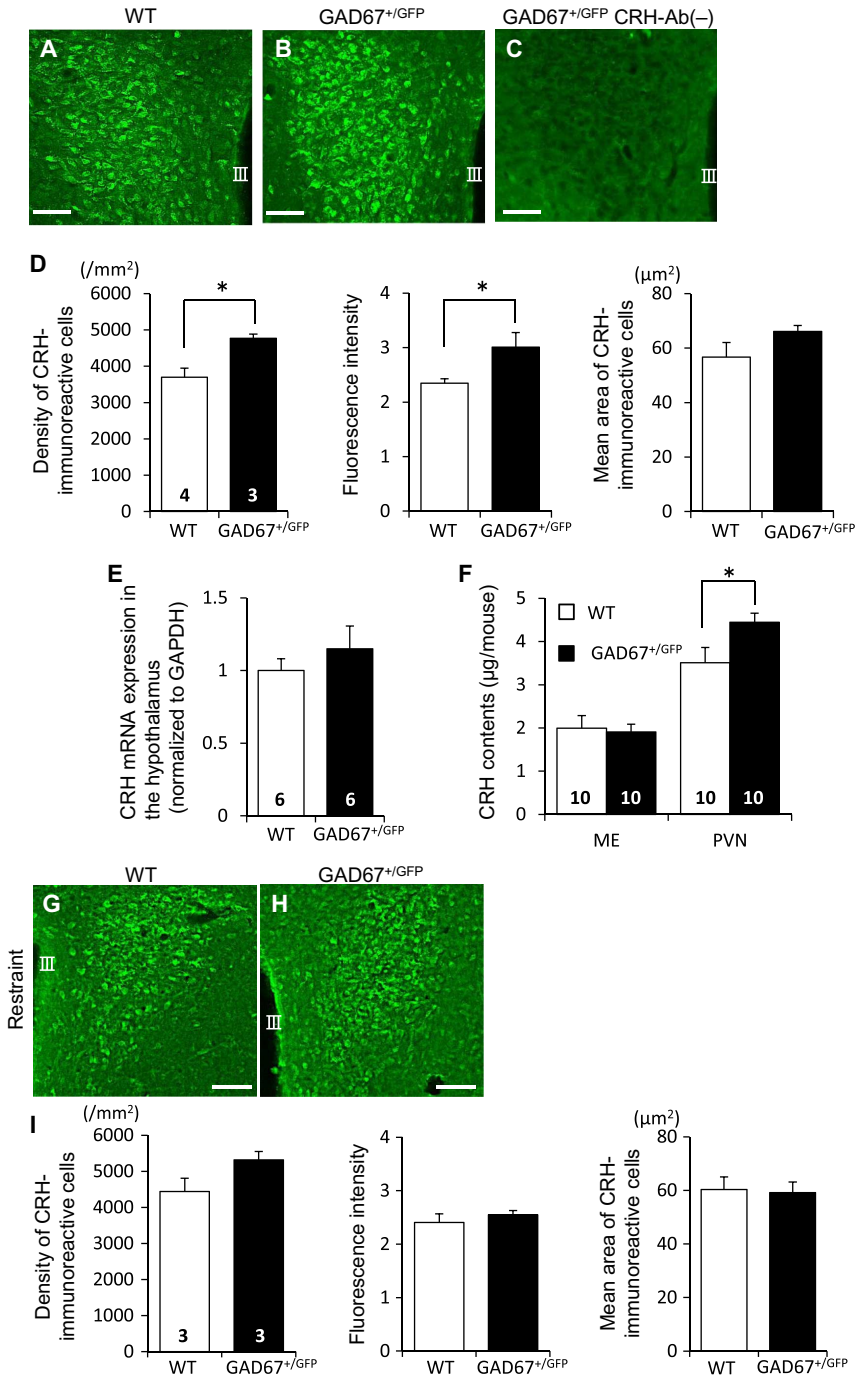

Fig. 2. CRH peptide accumulates in the cell bodies of the CRH neurons obtained from the GAD67$^{+/GFP}$ mice. (**A** and **B**) Representative immunofluorescence images of CRH in the PVN of the WT and GAD67$^{+/GFP}$ mice. III, third ventricle. (**C**) Antibody (Ab)–free negative control for CRH immunohistochemistry in the GAD67$^{+/GFP}$ mice. Note that no GFP fluorescence was observed within the PVN. Scale bars, 50 μm. (**D**) Quantitative analysis of the CRH-immunoreactive neurons. The fluorescence intensity represents the ratio of the intensities between the soma of the CRH neuron and the background. The density and fluorescence intensity of the CRH-immunoreactive cells in the PVN were significantly increased in the GAD67$^{+/GFP}$ mice compared with the values in the WT mice, whereas the mean areas of the CRH-immunoreactive cells were equivalent between the groups. (**E**) Quantitative real-time polymerase chain reaction (PCR) analysis indicated that the relative CRH mRNA expression in the hypothalamus was equivalent between the two groups. GAPDH, glyceraldehyde-3-phosphate dehydrogenase. (**F**) In GAD67$^{+/GFP}$ mice, the CRH content of the PVN, but not the content of the ME, was significantly increased relative to that of WT mice. (**G** and **H**) Representative immunofluorescence images of CRH in the PVN of the WT and GAD67$^{+/GFP}$ mice after a single 30-min bout of restraint-induced stress. Scale bars, 100 μm. (**I**) Quantitative analysis of the CRH-immunoreactive neurons after a bout of restraint stress. The density, fluorescence intensity, and mean area of the CRH-immunoreactive cells were all equivalent between the groups. *$P < 0.05$, Student's t tests between genotypes. Error bars represent SEM. The sample sizes are indicated within the bars.

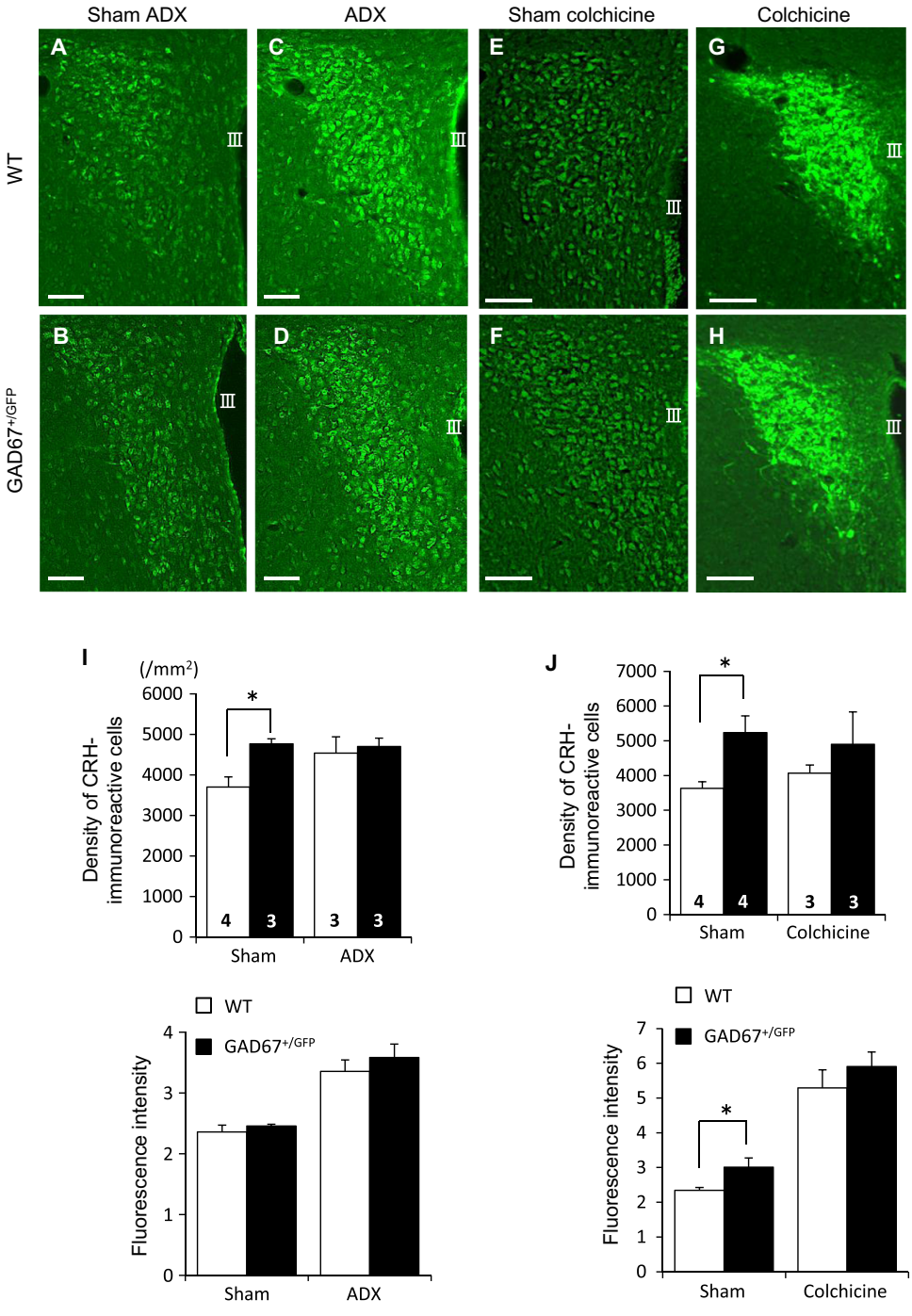

Fig. 3. Effects of ADX or an intracerebroventricular injection of colchicine on the CRH immunohistochemistry of adult WT and GAD67$^{+/GFP}$ mice. (**A** to **D**) Representative immunofluorescence images of CRH in the PVN of the WT and GAD67$^{+/GFP}$ mice at 12 days after the sham (A and B) or ADX (C and D) operation. (**E** to **H**) Representative immunofluorescence images of CRH in the PVN of the WT and GAD67$^{+/GFP}$ mice at 48 hours after the 0.9% saline (sham) (E and F) or colchicine (G and H) injections. Scale bars, 100 μm. (**I**) Following ADX, the density and the fluorescence intensity of CRH-immunoreactive cells in the PVN did not differ between the two groups. (**J**) Following the colchicine injection, the density and the fluorescence intensity of the CRH-immunoreactive cells in the PVN were equivalent between the two groups. *$P < 0.05$, Student's t tests between genotypes. Error bars represent SEM. The sample sizes are indicated within the bars.

wild type, 3.35 ± 0.19; GAD67$^{+/GFP}$, 3.58 ± 0.22; Fig. 3I). On the basis of these findings, we hypothesized that CRH peptide accumulation in the cell bodies of CRH neurons in GAD67$^{+/GFP}$ mice was a result of impaired CRH release. To test this hypothesis, we performed CRH immunohistochemistry on the PVN of adult mice that had been administered an intracerebroventricular injection of colchicine to inhibit the axonal transport of the peptide, which is synthesized in the cell body (Fig. 3, E to H). After 48 hours of intracerebroventricular colchicine inhibition, the density of the CRH-immunoreactive cells in the PVN was not significantly different between the genotype, and the fluorescence intensity of the CRH-immunoreactive cells in the PVN was increased to the same level in both genotypes (density: wild type, 4066.7 ± 233.3/mm^2; GAD67$^{+/GFP}$, 4900 ± 929.2/mm^2; intensity: wild type, 5.29 ± 0.52; GAD67$^{+/GFP}$, 5.91 ± 0.42; Fig. 3J). This finding suggests that the somatic accumulation of CRH in the GAD67$^{+/GFP}$ mice with reduced GABA levels may be a result of decreased levels of axonal transport, resulting from the impaired release of CRH from the axon terminal.

GABA$_A$R signaling affecting CRH release

To confirm whether the previously described findings were a result of reduced GABA synthesis in the GAD67$^{+/GFP}$ mice, we administered an intraperitoneal injection of muscimol, a GABA$_A$R agonist, and then analyzed the mice for any HPA axis alterations. Briefly, the brains were fixed for CRH immunohistochemistry, and plasma corticosterone and ACTH levels were measured 30 min after the muscimol (2 mg/kg in 0.9% saline) or vehicle (0.9% saline) injections. Following the muscimol injection, the density of detectable CRH-immunoreactive cells in the PVN was significantly decreased in the GAD67$^{+/GFP}$ mice, and the fluorescence intensity of the CRH-immunoreactive cells tended to decrease (density: vehicle, 3960 ± 65.5/mm^2; muscimol, 3470 ± 127.1/mm^2; $P < 0.01$, Student's t test; intensity: vehicle, 2.09 ± 0.04; muscimol, 1.87 ± 0.14). The mean areas of the CRH-immunoreactive cells were equivalent between the two groups (vehicle: 58.3 ± 2.1 μm^2; muscimol, 58.5 ± 1.7 μm^2; n = 5 to 6 mice per experimental group; Fig. 4, A to C). Furthermore, plasma corticosterone levels were significantly increased in the GAD67$^{+/GFP}$ mice following the muscimol injections, and plasma

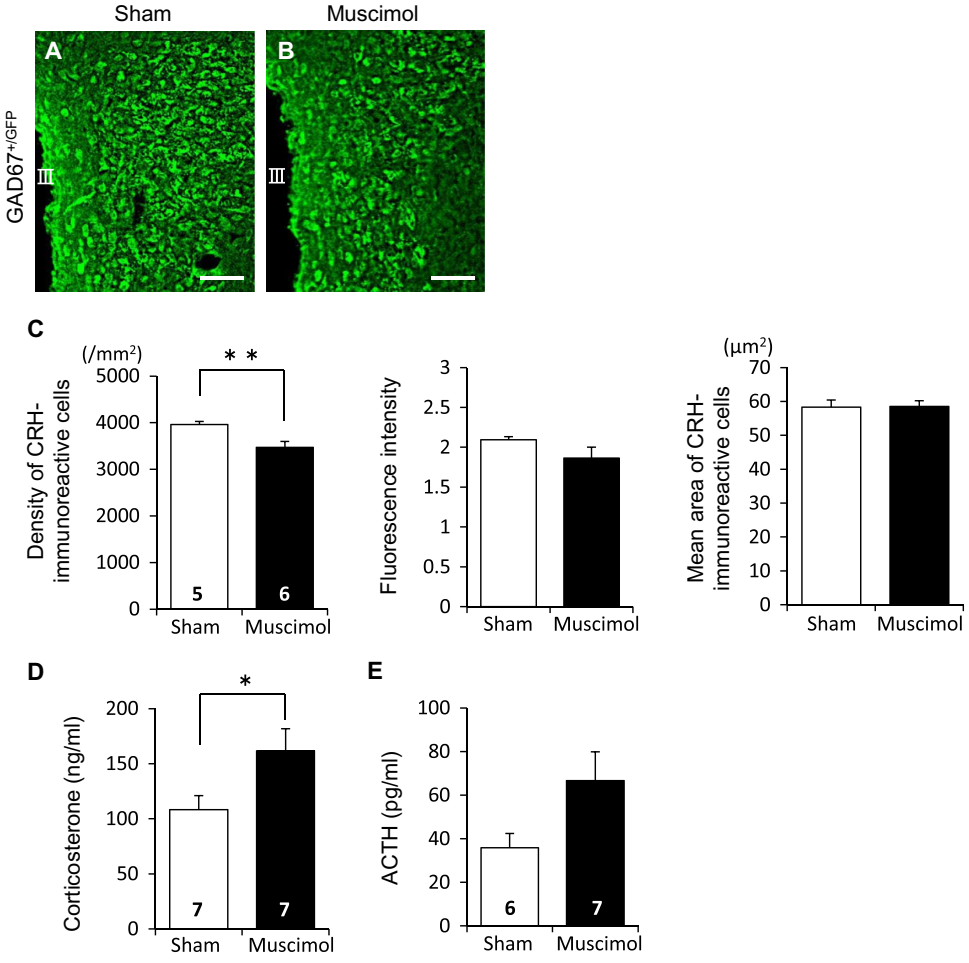

Fig. 4. Muscimol administration restored the accumulation of CRH in the GAD67$^{+/GFP}$ mice. (**A** and **B**) Representative immunofluorescence images of CRH in the PVN of the GAD67$^{+/GFP}$ mice at 30 min after a muscimol (2 mg/kg) or 0.9% saline (sham) injection. Scale bars, 50 μm. (**C**) Quantitative analysis of the CRH-immunoreactive neurons in the PVN. Following the muscimol injection, the density of the CRH-immunoreactive cells was significantly decreased, and the fluorescence intensity of the CRH-immunoreactive cells tended to decrease in the GAD67$^{+/GFP}$ mice. (**D** and **E**) Plasma corticosterone and ACTH levels in each group at 30 min after injection. Note that the muscimol treatment significantly increased plasma corticosterone levels in the GAD67$^{+/GFP}$ mice. *$P < 0.05$; **$P < 0.01$, Student's t tests. Error bars represent SEM. The sample sizes are indicated within the bars.

ACTH levels tended to increase (corticosterone: vehicle, 108.4 ± 12.6 ng/ml; muscimol, 161.7 ± 20.0 ng/ml; $P < 0.05$, Student's t test; ACTH: vehicle, 35.9 ± 6.5 pg/ml; muscimol, 66.6 ± 13.2 pg/ml; $n = 6$ to 7 mice per experimental group; Fig. 4, D and E). Plasma corticosterone levels were significantly increased in the wild-type mice following the muscimol injections, and plasma ACTH levels tended to increase, whereas this treatment failed to decrease the density of the CRH-immunoreactive cells (fig. S2, A to E). Thus, muscimol may have an excitatory function in the terminals of CRH neurons, and this $GABA_AR$ activation restored the somatic CRH levels in the $GAD67^{+/GFP}$ mice back to that in the wild-type mice.

Existence of GABAergic terminals and $GABA_ARs$ on the axon terminals of CRH neurons in the ME and the retrograde labeling of the arcuate nucleus

In $GAD67^{+/GFP}$ mice, the GFP (GAD67)–positive nerve terminals were present in close proximity to the CRH-positive nerve terminals in the ME, and the GFP-labeled GABAergic neurons were located on the periphery of the cluster of the CRH-immunoreactive neurons in the PVN (Fig. 5, A to F). In addition, the vesicular GABA transporter (VGAT)–immunoreactive axon varicosities were juxtaposed onto the somata and axon terminals of the CRH neurons (Fig. 5, G to L). The CRH neurons expressed $GABA_AR$ in both their somata and axon terminals (Fig. 5, M to R). Thus, GABAergic innervations were present in the somata and the axon terminals of the CRH neurons. According to previous studies, the origins of the GABAergic inputs to the ME are primarily from the arcuate nucleus (ARC) (*16*, *19*, *20*). To confirm the origin of the GABAergic inputs to the terminals of the CRH neurons in the animals in our study, we performed intraperitoneal injections of Fluoro-Gold in $GAD67^{+/GFP}$ mice to trace the projections to the ME in a retrograde manner (*21*). Four days after Fluoro-Gold injection, Fluoro-Gold fluorescence was detected in the PVN and the ARC. GFP-expressing GABAergic cells in the ARC, but not in the suprachiasmatic nucleus (SCN) or the dorsomedial hypothalamus (DMH), were labeled with the injected Fluoro-Gold (Fig. 6). These results demonstrate that GABAergic inputs from the ARC to the ME and the terminals of the CRH neurons exist.

Enhancement of persistent CRH release from the axon terminals in the ME via excitatory GABAergic effects

GABA is required to depolarize the postsynaptic membrane potential to facilitate CRH release. Therefore, the $[Cl^-]_i$ must be sufficiently high to positively shift the GABA reversal potential beyond the action potential threshold. Thus, we examined the expression patterns of the KCC2 and the Na^+-K^+-$2Cl^-$ (NKCC1) cotransporters, which are both membrane-bound transport proteins responsible for establishing the Cl^- gradient in neurons. KCC2 extrudes K^+ and Cl^- from the cell, and NKCC1 imports Na^+, K^+, and $2Cl^-$ into the cell across the plasma membrane. In double immunostaining experiments using antibodies for CRH and KCC2 (Fig. 7, A to F) or NKCC1 (Fig. 7, G to L), NKCC1, but not KCC2, was expressed in the CRH neuron terminals in the ME. In contrast, the somata of the CRH neurons were enriched with KCC2 but not with NKCC1. These findings suggest that the $[Cl^-]_i$ is increased at the CRH nerve terminals relative to the concentration in the cell body, which is a result of the expression patterns of NKCC1 and KCC2 and leads to the excitatory actions of GABA on the terminals of the CRH neurons in the ME.

To elucidate the GABA-mediated excitation in the terminals of the CRH neurons, we performed calcium (Ca^{2+}) imaging in the PVN and

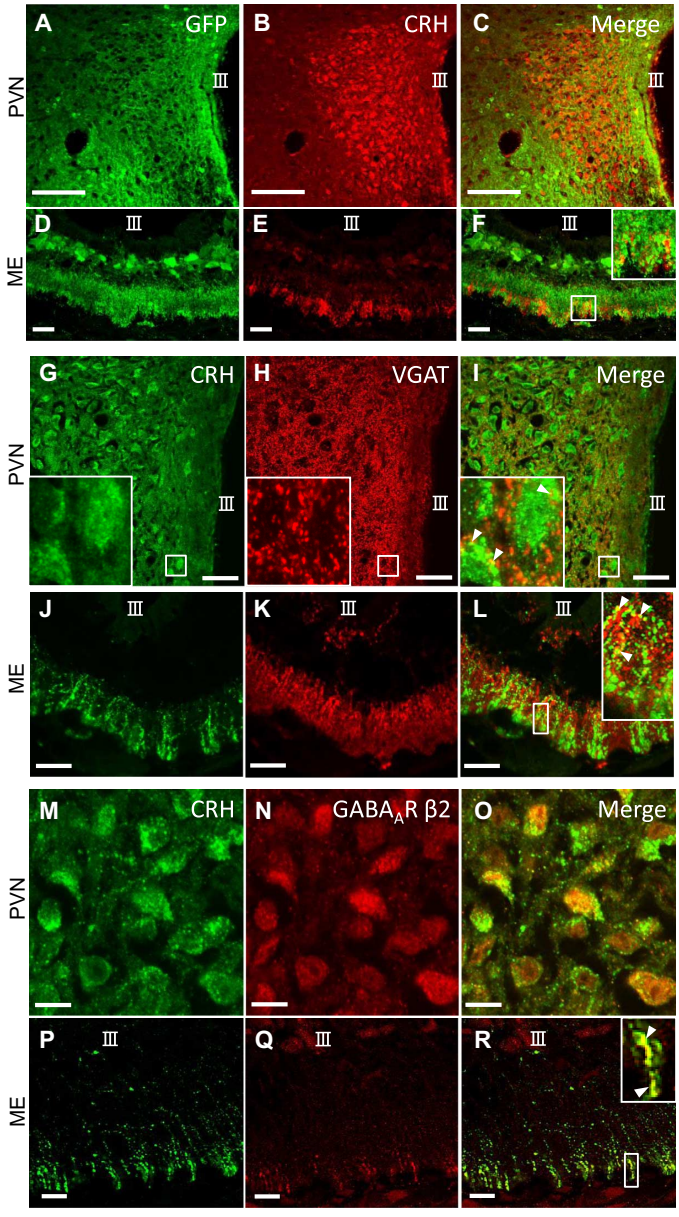

Fig. 5. GABAergic inputs are present on the axon terminals of the CRH neurons in the ME. (**A** to **F**) Representative confocal images of the PVN (A to C) and the ME (D to F) from the $GAD67^{+/GFP}$ mice immunostained for GFP (left; green) and CRH (middle; red) demonstrate that the two proteins were colocalized in the ME (right; yellow) (F). The GABAergic neuronal somata in the ARC were also observed in the periphery of the third ventricle (D and F). In the PVN, the GFP-labeled GABAergic neurons were located on the outside of a cluster of CRH-immunoreactive neurons (C). (**G** to **R**) The representative confocal images of the PVN and ME of the WT mice immunostained for VGAT (middle; red) (H and K), the $GABA_AR$ β2 subunit (middle; red) (N and Q), and CRH (left; green) demonstrate that VGAT and $GABA_AR$ colocalized with CRH in both the PVN and the ME (right; yellow). The arrowheads in the insets indicate the colocalization of CRH with VGAT (I and L) or with the $GABA_AR$ β2 subunit (O and R). For all insets, the boxed areas are shown at a higher magnification (×4). Scale bars, 100 μm (A to C), 20 μm (D to L), and 10 μm (M to R).

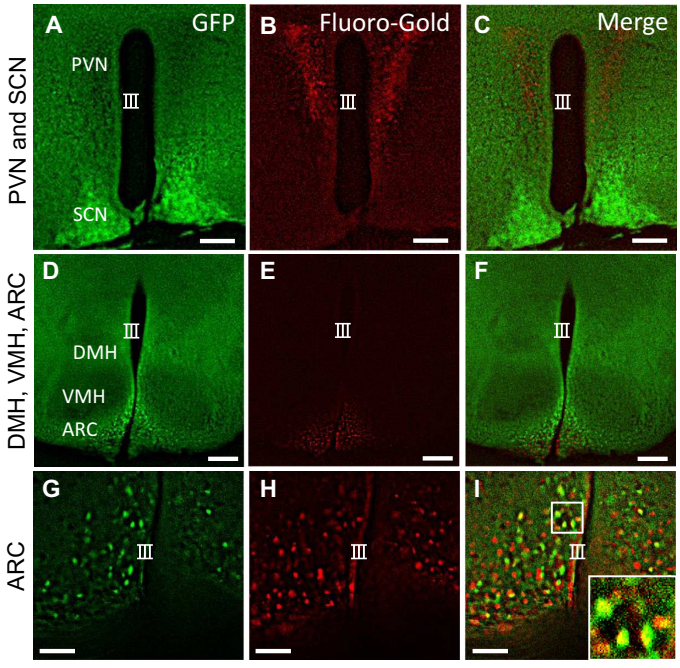

Fig. 6. GABAergic inputs to the ME originate from the ARC. (**A** to **I**) Representative fluorescence images of the PVN and SCN (A to C); the DMH, VMH (ventromedial hypothalamus), and ARC (D to F); and the ARC (G to I) from the GAD67$^{+/GFP}$ mice based on GFP (left; green) and Fluoro-Gold (middle; red) visualization. The GABAergic cells in the ARC (F and I), but not in the SCN and DMH (C and F), were retrogradely labeled by Fluoro-Gold. For the inset, the boxed area is shown at a higher magnification (×4). Note that the neuroendocrine cells in the PVN were also retrogradely labeled by Fluoro-Gold (B). Scale bars, 100 μm (A to C), 200 μm (D to F), and 50 μm (G to I).

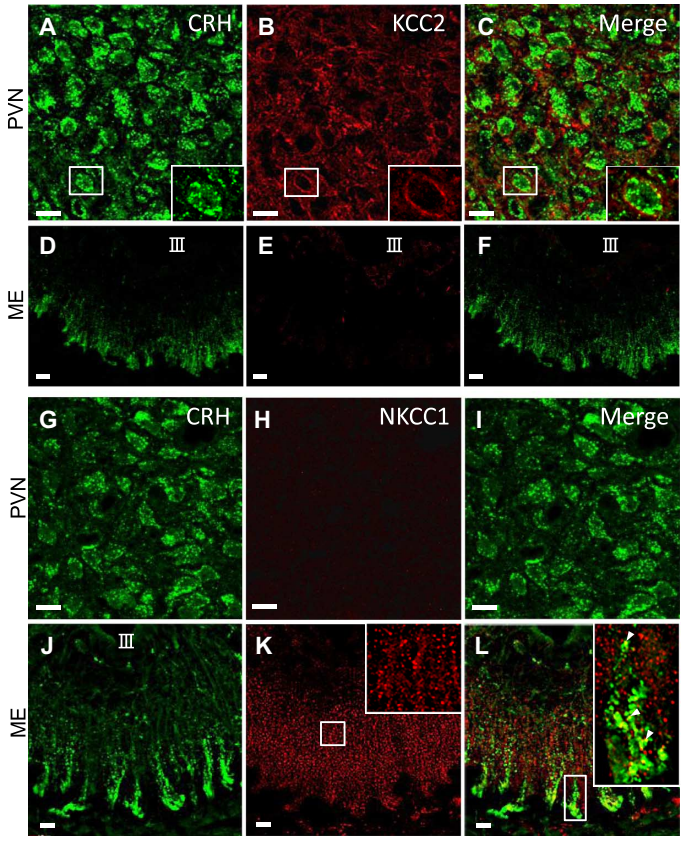

Fig. 7. NKCC1 and KCC2 expression patterns in the CRH neurons of the PVN and ME. (**A** to **F**) Representative confocal images of the PVN (A to C) and the ME (D to F) of the WT mice immunostained for CRH (left; green) and KCC2 (middle; red). KCC2 was identified in the somata of the CRH neurons (B and C) but not in the axon terminals of the CRH neurons in the ME (E and F). (**G** to **L**) Representative confocal images of the PVN (G to I) and ME (J to L) of the CRH-Venus mice immunostained with anti-GFP (left; green) and anti-NKCC1 (middle; red) antibodies. Note the dot-like immunostaining for NKCC1 in the ME (K). The arrowheads indicate the colocalization of CRH and NKCC1 in the ME (inset) (L). In contrast, NKCC1 was not identified in the somata of the CRH neurons in the PVN (H and I). For all insets, the boxed areas are shown at higher magnifications [×2.5 (A to C) and ×4 (K and L)]. Scale bars, 10 μm.

the ME of CRH-GCaMP3 mice. CRH-specific GCaMP3 expression in both the PVN and the ME was achieved by crossing the Ai38 reporter mice with the CRH-iCre mice (Fig. 8, A to F). With acute sections from the brains of CRH-GCaMP3 mice, the application of muscimol (10 μM) to the somata of the CRH neurons in the PVN induced decreases in the intracellular calcium concentration $[Ca^{2+}]_i$ (Fig. 8, G to I). At the CRH terminals in the ME, muscimol produced an increase in the $[Ca^{2+}]_i$ (Fig. 8, J to L), which is in contrast to the decreases identified in the somata in the PVN (n = 23, four PVNs from four CRH-GCaMP3 mice; n = 5, five MEs from five CRH-GCaMP3 mice). The $[Ca^{2+}]_i$ responses to the high-K^+ (50 mM) solution in the ME were weak and slow compared with the responses in the PVN, and the high-K^+–induced increase in $[Ca^{2+}]_i$ was nearly equivalent to that of the muscimol-induced $[Ca^{2+}]_i$ ($\Delta F/F$; PVN: muscimol, −16.9 ± 2.4%; K^+, 106.7 ± 17.9%; ME: muscimol, 16.8 ± 1.9%; K^+, 21.3 ± 1.6%; Fig. 8M). These findings indicate that GABA is excitatory at the CRH terminals in the ME but inhibitory on the CRH neuronal somata in the PVN under nonstressful conditions. We subsequently used a two-photon microscope to perform a more detailed observation of the Ca^{2+} transients in the CRH axon terminals (Fig. 9, A and B). The muscimol-induced increased $[Ca^{2+}]_i$ levels were significantly attenuated by the application of the NKCC1 inhibitor bumetanide (10 μM) ($\Delta F/F$; muscimol, 14.2 ± 1.8%; muscimol + bumetanide, 4.6 ± 1.0%; n = 9, three clusters of CRH neuronal terminals per section, three sections per CRH-GCaMP3 mouse; $P < 0.001$, Student's t test; Fig. 9, C to E). Because the repeated application of muscimol did not cause a significant rundown of its response, these findings indicate that the excitatory effects of GABA rely on the high $[Cl^-]_i$ produced by the NKCC1 expressed in the CRH terminals in the ME.

The excitatory GABA-mediated effect on CRH axon terminals involved in steady-state CRH release

On the basis of the results of the acute stress experiments (Figs. 1 and 2), we hypothesized that the excitatory effects of GABA at the ME are primarily responsible for mediating the steady-state release of CRH but are not involved in the acute stress–induced response. Finally, we tested this hypothesis using intraperitoneal administration of bumetanide,

which is thought to work at the ME, but not at the PVN (see Figs. 7 and 9 and fig. S3), followed by a bout of acute restraint-induced stress. Briefly, wild-type mice received either bumetanide (30 mg/kg) or vehicle (0.9% saline) 15 min before a single 30-min bout of restraint-induced stress; then, their brains were fixed for CRH immunohistochemistry, and plasma samples were collected. The CRH immunoreactivity parameters in the PVN (density: vehicle, 4294.4 ± 74.7/mm^2; bumetanide, 4455.4 ± 212.1/mm^2; intensity: vehicle, 2.22 ± 0.11; bumetanide, 2.58 ± 0.07; area: vehicle, 55.6 ± 2.5 μm^2; bumetanide, 60.2 ± 1.9 μm^2) were equivalent between the groups (n = 6 mice per experimental group; Fig. 10, A to C). Plasma corticosterone and ACTH levels (corticosterone: vehicle, 93.7 ± 7.77 ng/ml; bumetanide, 110.0 ± 18.7 ng/ml; ACTH: vehicle, 648.7 ± 44.4 pg/ml; bumetanide, 811.9 ± 73.8 pg/ml) were also equivalent between the two groups (n = 6 mice per experimental group; Fig. 10, D and E). In addition, the expression patterns for KCC2 and NKCC1 in the CRH neurons were not altered after acute restraint-induced stress (fig. S3, A to L). These findings suggest that the excitatory GABA-mediated CRH release from the ME may not be responsible for an acute stress–induced response.

DISCUSSION

Our findings demonstrate that GABA$_A$R-mediated signaling facilitates CRH release from the axon terminals of CRH neurons in the ME. This excitatory action of GABA at the axon terminal is the opposite of its action at the somata of CRH neurons in the PVN, where the GABAergic inputs inhibit CRH neurons (*3*, *5*, *6*). To our knowledge, this is the first study to demonstrate that GABA has physiological actions at the terminals of CRH neurons, that is, the promotion of CRH release via excitatory GABA$_A$R activation. Thus, our findings demonstrate a novel mechanism for controlling the HPA axis and/or energy metabolism via presynaptic GABAergic actions in the ME, in addition to the classical GABAergic mechanism at the level of the PVN (fig. S4).

In GABA-deficient GAD67$^{+/GFP}$ mice, the injection of muscimol, a GABA$_A$R agonist, restored the increased density and fluorescence intensity of the CRH-immunoreactive cells in the PVN, which indicates the accumulation of somatic CRH. In addition, this treatment increased plasma corticosterone and ACTH levels. In GAD67$^{+/GFP}$ mice, CRH release is decreased because of a reduced release of GABA at the CRH terminal. Therefore, these findings are compatible with the hypothesis

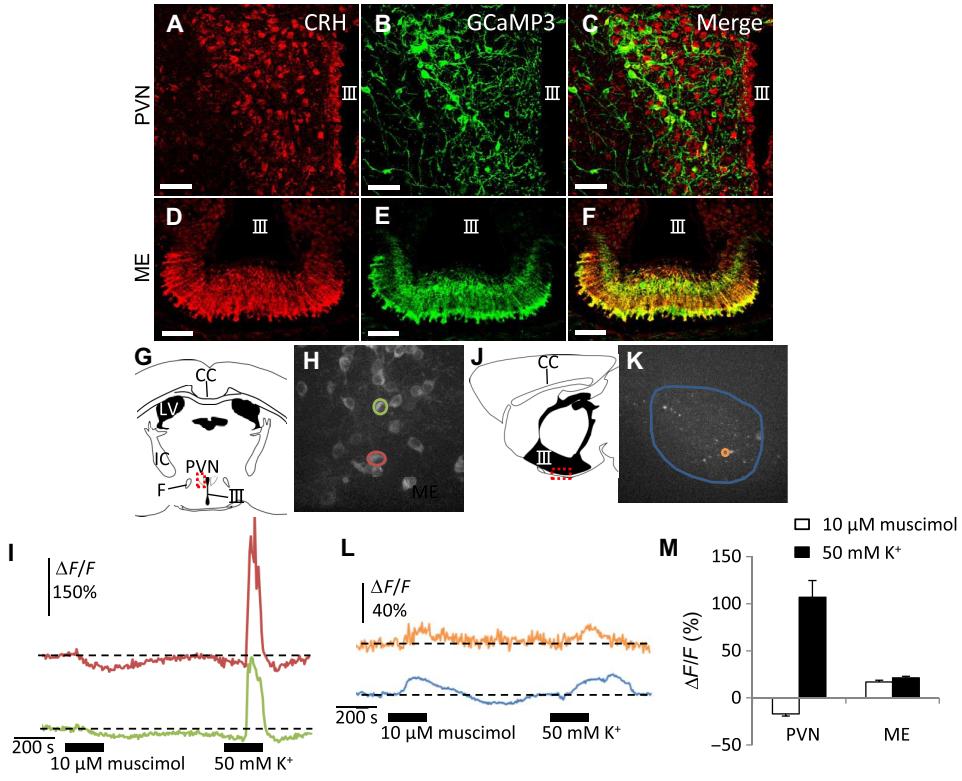

Fig. 8. GABA-evoked increases in the $[Ca^{2+}]_i$ in the axon terminals of the CRH neurons in the ME. (**A** to **F**) Representative confocal images of the PVN (A to C) and ME (D to F) of the CRH-GCaMP3 mice immunostained for CRH (left; red) and GCaMP3 (middle; green). Note that all GCaMP3-immunoreactive cell bodies and fibers were also immunoreactive for CRH (right; yellow). Scale bars, 50 μm. (**G**) Illustration of the PVN in a coronal brain section. LV, lateral ventricle; IC, internal capsule; F, fornix. (**H**) Representative fluorescence image of GCaMP3 in the soma of a CRH neuron in the PVN during the experiment. Scale bars, 30 μm. (**I**) Fluorescence responses recorded from the cells indicated in (H). (**J**) Illustration of the ME in a sagittal brain section. CC, corpus callosum. (**K**) Representative fluorescence image of GCaMP3 in an axon terminal from a CRH neuron in the ME during the experiment. The regions of interest (ROIs) corresponded to a fluorescent spot (orange) and a wide area of the ME (blue). Scale bar, 30 μm. (**L**) The fluorescence changes recorded from the terminals in the ROIs indicated in (K) show that the fluorescence responses in the fluorescent spot (upper trace; orange) and a larger area of the ME (lower trace; blue) were similar. (**M**) Peak $[Ca^{2+}]_i$ changes in response to 10 μM muscimol and 50 mM K^+ in the PVN and the ME, which indicate that GABA may excite the terminals of the CRH neurons in the ME but inhibit the somata of the CRH neurons in the PVN (soma: n = 23, four PVNs from four CRH-GCaMP3 mice; terminals: n = 5, five MEs from five CRH-GCaMP3 mice).

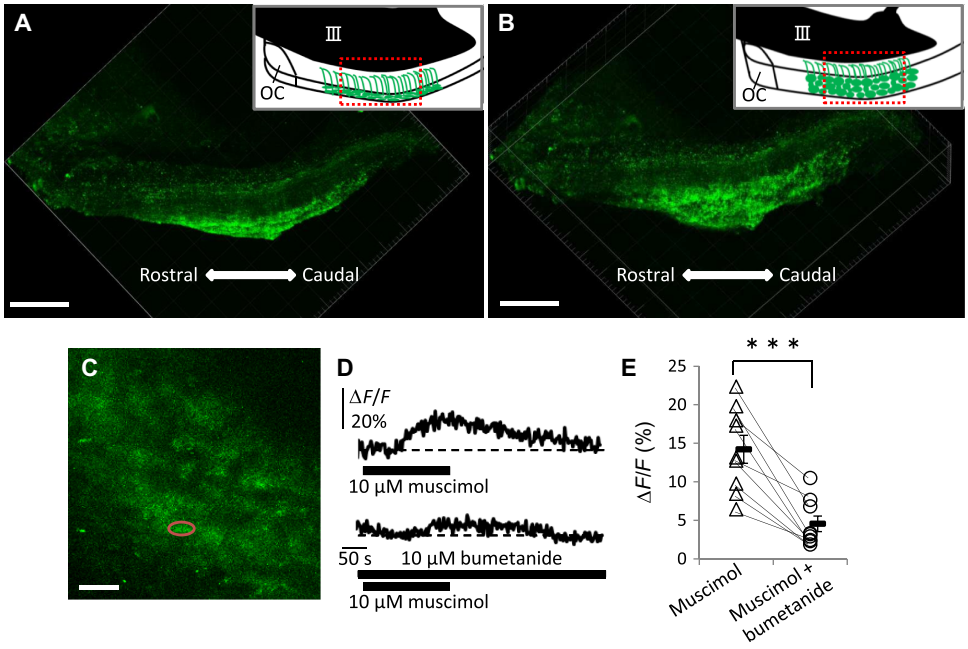

Fig. 9. The GABA-induced increase in the $[Ca^{2+}]_i$ in the terminals of the CRH neurons is attenuated by an NKCC1 inhibitor. (**A**) Three-dimensional reconstruction from the stacked images of the ME in the CRH-GCaMP3 mice obtained from a two-photon microscope. OC, optic chiasm. (**B**) Laterally rotated image in (A). Clusters of CRH-positive axon terminals were identified at the bottom of the ME. Scale bar, 100 μm. (**C**) Representative high-magnification fluorescence image of GCaMP3 in the ME. The ROI corresponds to a single cluster of CRH-positive axon terminals. Scale bar, 20 μm. (**D**) Fluorescence changes recorded from the ROI indicated in (C). The muscimol-induced increase in the $[Ca^{2+}]_i$ was attenuated by the NKCC1 inhibitor bumetanide. (**E**) The peak $[Ca^{2+}]_i$ responses to muscimol recorded from single terminal clusters in the ME indicate that the excitatory actions of GABA rely on the high $[Cl^-]_i$ produced by NKCC1 in CRH-positive axon terminals ($n = 9$, three clusters of CRH axon terminals per section, three sections per CRH-GCaMP3 mouse). ***$P < 0.001$, Student's *t* tests. Error bars represent SEM.

described above because muscimol appears to supplement the decreased excitatory effects of GABA in the ME in this strain of mice. We found that the plasma corticosterone and ACTH levels in the wild-type mice responded to muscimol in a manner similar to the $GAD67^{+/GFP}$ mice (fig. S2), suggesting that GABA may also have excitatory effects at the terminals of CRH neurons in wild-type mice. GAD67 and GAD65 both synthesize GABA. However, GAD67 is predominant in immature animals, and in the adult brain, its activity is restricted to extrasynaptic GABA, which is involved in tonic inhibition (*22*, *23*). Tonic inhibition plays an important role in the GABAergic control of CRH neurons in the PVN in response to acute stress (*12*, *24*). Because GAD67 was found to be abundant at the CRH terminals in the ME, the tonic activation of $GABA_AR$ in the ME, that is, its depolarization, may also be involved in steady-state CRH release.

The inhibitory actions of GABA rely on the relatively low $[Cl^-]_i$ maintained by KCC2 in mature neurons (*10*). In contrast, GABA exhibits excitatory actions in immature neurons because NKCC1 predominates (*25*, *26*). Here, using adult mice, we demonstrated that NKCC1, but not KCC2, was expressed in the CRH terminal in the ME, whereas the somata of the CRH neurons were enriched with KCC2 but not with NKCC1. This differential expression of KCC2 and NKCC1 may result in the differences in $[Cl^-]_i$; thus, GABA may cause excitation at the terminals (*27*–*29*). Therefore, the $GABA_AR$-mediated effects at the CRH axon terminals may be excitatory and facilitate CRH release from the ME. Turecek and Trussell (*30*) demonstrated for the first time that an increased $[Cl^-]_i$ in the axon terminals relative to that in the somata causes depolarization and enhances transmitter release at a mammalian central synapse via the presynaptic glycine receptor at the calyceal synapse in the medial nucleus of the trapezoid body. Jang *et al.* (*28*) also demonstrated that presynaptic $GABA_AR$ activation at glutamatergic nerve terminals in CA3 hippocampal neurons facilitates glutamate release. The $[Cl^-]_i$ in axon terminals is estimated to be approximately 20 mM (*31*, *32*), and the mechanism of Cl^- accumulation in the terminal, which is independent of the somatic mechanism, is thought to be mediated by NKCC1 in glutamatergic terminals in the ventromedial hypothalamic nucleus (*27*), trigeminal nerve terminals (*33*), and sciatic nerve terminals (*34*), but by other mechanisms in the calyx of Held (*32*).

$GABA_AR$-mediated depolarization with high $[Cl^-]_i$ in the terminals of the posterior pituitary inhibits hormone secretion (*31*, *35*). The degree of depolarization determines whether transmitter release is facilitated or inhibited, and it is regulated by $[Cl^-]_i$. Subthreshold depolarization inhibits transmitter release via the inactivation of voltage-dependent Na^+ and/or Ca^{2+} channels (*31*, *36*) or by shunting the initiation of the action potential through $GABA_AR$-mediated Cl^- conductance, thus depolarizing the primary sensory afferents of the trigeminal and spinal sensory nerves, which is most likely a result of a subthreshold GABA reversal potential with a moderately increased $[Cl^-]_i$ (*33*, *37*, *38*). Facilitation is caused by a small depolarization that activates the voltage-gated Ca^{2+} channels and increases the resting intraterminal Ca^{2+} concentrations (*30*, *39*); larger depolarizations generate action potentials accompanied by Ca^{2+} influx (*27*, *28*, *33*). Regarding the latter mechanism, the expression and/or up-regulation of NKCC1 in the primary trigeminal sensory terminals (*33*)

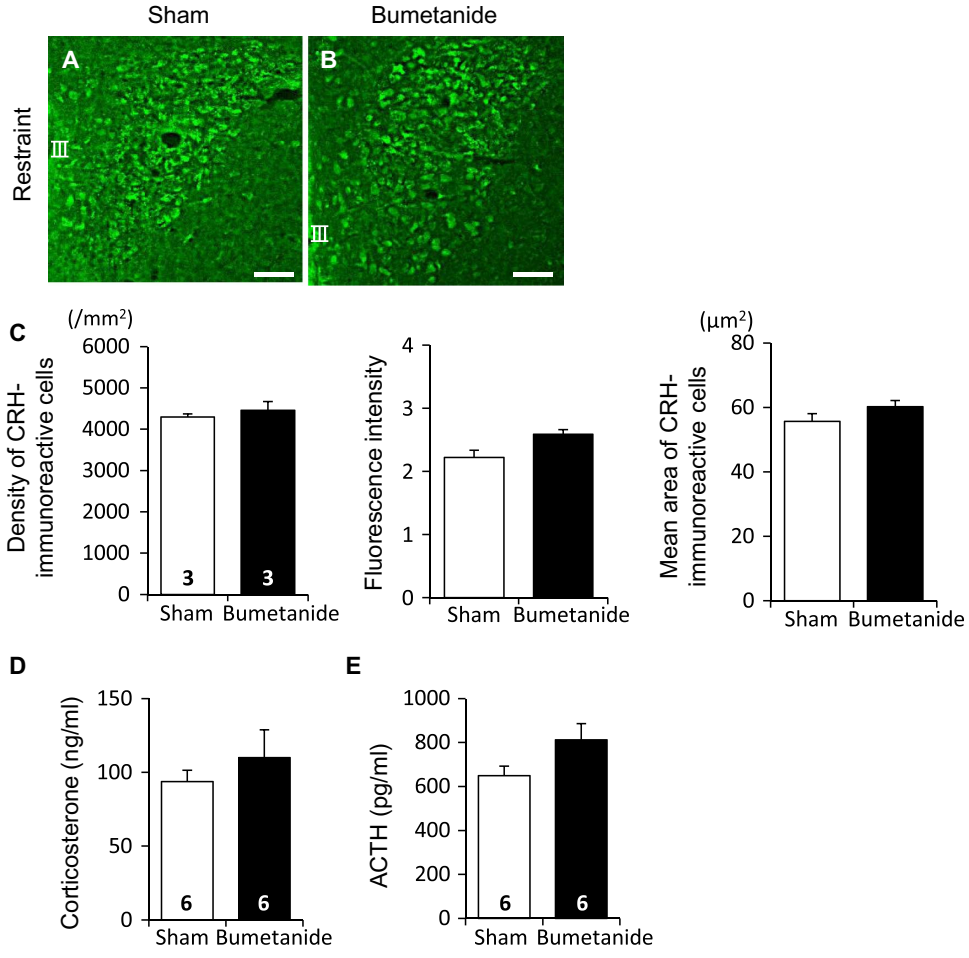

Fig. 10. Bumetanide administration did not alter HPA axis parameters following acute stress. (**A** and **B**) Representative immunofluorescence images of CRH in the PVN of the WT mice after a bumetanide (30 mg/kg) or 0.9% saline (sham) injection followed by a single 30-min bout of restraint-induced stress. Scale bars, 50 μm. (**C**) Quantitative analysis of the CRH-immunoreactive neurons. The density, fluorescence intensity, and mean area of the CRH-immunoreactive cells were all equivalent between the groups. (**D** and **E**) Plasma corticosterone and ACTH levels in each group. Both corticosterone and ACTH levels were equivalent between the two groups. Error bars represent SEM. The sample sizes are indicated within the bars.

and in the glutamatergic nerve terminals in the VMH (*27*) and CA3 region of the hippocampus (*28*) are critical. Bumetanide, an NKCC1 inhibitor, which causes a complete lack of active Cl^- uptake and decreases the $[Cl^-]_i$ down to a passive equilibrium level (*40*), reversed the muscimol-evoked Ca^{2+} transients in the ME (Fig. 9); thus, $GABA_AR$ mediated excitation in the CRH neuronal terminals in response to the Cl^- efflux–mediated depolarization. Despite opposite $[Ca^{2+}]_i$ transients at the somata and the terminals of CRH neurons, our conclusion that GABA acts inhibitory in the PVN but excitatory in the ME has limitations without direct measurements of muscimol-evoked potentials. Thus, a future study is still required to prove differential actions of $GABA_AR$-mediated synaptic potentials from identified CRH neurons, although Sarkar *et al.* (*12*) reported hyperpolarizing inhibitory postsynaptic potentials in the somata of identified CRH neurons from nonstressful mice.

Although there are some discrepancies between the gene and protein expression levels in some models using genetic ablation techniques (*41*), in our CRH-iCre mice crossed with CAG-CAT-EGFP transgenic mice, most EGFP (enhanced GFP) neurons (85 ± 2%) coexpress CRH in the PVN (*42*). Thus, we are convinced that GCaMP3 is expressed specifically in CRH neurons in CRH-iCre:Ai38 mice (CRH-GCaMP3 mice). In addition, we generated GAD67-GFP knock-in mice using a gene-targeting method that involved homologous recombination in embryonic stem cells (*14*). Because both the GFP and GAD67 genes in the knock-in mice are identically controlled, the parallel GFP protein expression accurately reflects GAD67 expression in hypothalamic GABAergic neurons (*20*).

Because the origins of the afferent GABAergic inputs are different between the parvocellular PVN [for example, the anterior perifornical region, anterior hypothalamic area ventral to the PVN, perinuclear zone of the supraoptic nucleus, the rostral region of the PVN itself, and the bed nucleus of the stria terminals; (*5*–*9*)] and the ME [that is, ARC; (*20*)], the physiological functions of these afferent GABAergic inputs may also contribute to the differential control of the CRH neurons between the PVN and the ME. Under acute stressful conditions, corticosterone, which is a stress hormone in rodents, is rapidly released into the blood to adapt to the condition (*43*). Acute stress converts the effects of GABA on CRH neurons from inhibitory to excitatory, which

is mediated by the increase in $[Cl^-]_i$. This process requires the phosphorylation and subsequent internalization of KCC2 (*11*, *12*). Chronic stress also decreases the GABAergic inhibition of CRH neurons via the suppression of KCC2 activity in the PVN, and it induces depression-like behavior (*13*). Therefore, the excitatory action of GABA at the axon terminals of CRH neurons must also be considered an additional mechanism that controls the HPA axis in response to acute and chronic stress. However, on the basis of the results of our acute stress experiments, we hypothesized that excitatory GABA-mediated CRH release from the ME may be involved primarily in the steady-state release of CRH, in contrast to the effects in the PVN (*11*, *12*). Here, we did not examine the effects of chronic stress. Therefore, future studies are required to address the role of GABA in the ME during chronic stress.

Chronic HPA axis hyperactivity is considered an important molecular mechanism underlying the pathology of major depressive disorders (*44*), which affect appetite in many cases. Because the ARC, where the GABAergic inputs to the ME originate, controls food intake (*45*) and energy homeostasis, persistent HPA axis stimulation in the ME via excitatory GABA effects may affect appetite and/or energy balance via reciprocal actions between anorexigenic (for example, leptin and CRH) and orexigenic [for example, neuropeptide Y (NPY)] factors as a part of a regulatory loop in energy homeostasis via the PVN and ARC (*46*). With regard to this process, the reciprocal regulation of KCC2 and NKCC1 by the with-no-lysine protein kinase (WNK) and the downstream STE20/SPS1-related proline/alanine-rich kinase (SPAK)/oxidative stress responsive kinase 1 (OSR1) pathways (*47*, *48*) may play pivotal roles in these GABAergic regulatory effects because KCC2 and NKCC1 are the key molecules that determine GABAergic actions in the PVN (*11*, *12*) and ME (Figs. 7 to 9), respectively. Notably, patients with schizophrenia have been shown to have increased levels of both OSR1 and WNK3 mRNA (*49*).

For processes that are not responsive to acute stress, the modulation of steady-state CRH release may be involved, such as the regulation of energy metabolism (*50*) and/or feeding (*46*). The ARC integrates synaptic information and endocrine signals from the blood, which is facilitated by the localized weakness of the blood-brain barrier (*20*). In the ARC, several types of neurons, for example, pro-opiomelanocortin (POMC) neurons, agouti-related protein (AgRP) neurons, and rat insulin II gene promoter (RIP)–expressing neurons, monitor energy status and modulate behavioral and metabolic responses (*51*, *52*). Of these neurons, AgRP neurons expressing glucocorticoid receptors and RIP neurons expressing leptin receptors are both GABAergic (*51*, *52*). A loss of GABA release from RIP GABAergic neurons can cause obesity via the PVN non-neuroendocrine cells projecting to nucleus tractus solitarius (*52*). GABAergic RIP neurons in the ARC appear to project to the ME (*52*). A previous study indicated that intracerebroventricular injection of leptin increased hypothalamic CRH synthesis but did not increase serum corticosterone levels (*46*). This discrepancy may be explained by the present result if leptin inhibits ME-projecting RIP neurons. A portion of the non–PVN-projecting RIP neurons is inhibited by leptin (*52*). Therefore, leptin-mediated changes in CRH release may be attributable to excitatory GABAergic input from the ARC to the CRH neuronal terminals in the ME, which we have reported here. The AgRP GABAergic neurons coexpress NPY and thus play a counteracting role against RIP GABAergic neurons in the regulation of energy metabolism, although both are the first to respond to circulating signals (*51*, *52*). NPY released by local axons modulates neuroendocrine regulation, including CRH (*20*). Both NPY and peptide YY acting as a long-distance signal from the gut inhibit antidromically identified ME-innervating GABAergic neurons in the ARC (*20*). This process may represent an inhibitory endocrine system that acts via hormonal monitoring in the ARC, reducing the release of CRH at the ME.

In summary, we report a novel mechanism by which the effects of GABA promote persistent CRH secretion from the axon terminals of the CRH neurons in the ME. This mechanism acts via a $GABA_AR$-mediated excitatory signal that has been reported in many brain structures at different developmental stages including in vivo (*53*). Previous studies have indicated that $GABA_AR$ activation of gonadotropin-releasing hormone (GnRH) neuronal somata produces depolarizations and initiates action potentials (*54*, *55*). Thus, future studies are required to address the GABAergic actions at the axon terminals of GnRH neurons, as well as the other hypothalamic neuroendocrine terminals in the ME. In addition, a detailed mechanistic analysis of CRH-terminal Cl^- homeostasis with respect to GABAergic controls originating from the ARC is an important and feasible goal because genetically encoded Cl indicator lines of mice controlled by Cre recombination are available (*56*, *57*). Our findings regarding the differences in GABA action between the somata and axonal terminals of CRH neurons with differential Cl^- homeostasis may assist in the development of treatments for psychiatric and metabolic disorders caused by malfunctions of GABAergic neurons interconnecting the PVN-ARC-ME triangle (fig. S4).

MATERIALS AND METHODS

Animals

We used female and male $GAD67^{+/GFP}$ mice and their wild-type controls of the same genetic background (wild-type mice, C57BL/6). The generation of the $GAD67^{+/GFP}$ mice has been previously described (*14*). The mice were housed in a cage under a 12-hour light-dark cycle (lights off from 1900 to 0700) and were allowed free access to drinking water and food pellets. Pairs of adult female wild-type mice and male $GAD67^{+/GFP}$ mice were housed together in a cage overnight. The day on which a vaginal plug was identified after a morning inspection was designated as E0.5. Cre-dependent GCaMP3 reporter mice ("Ai38," The Jackson Laboratory, stock no. 014538) (*58*), CRH-iCre mice, and CRH-Venus mice (*42*) were also used. Pairs of mice with heterozygous CRH-iCre and Ai38 genotypes were mated, and the heterozygous CRH-iCre:Ai38 offspring (CRH-GCaMP3 mice) were used for Ca^{2+} imaging. In addition, pairs of heterozygous CRH-iCre mice were mated, and the homozygous CRH-iCre embryos were used to evaluate the specificity of an anti-CRH primary antibody. PCR amplification was performed to discriminate the genotypes of the individuals. All experiments were performed in accordance with the guidelines issued by the Hamamatsu University School of Medicine for the ethical use of animals for experimentation, and all efforts were made to minimize the number of animals used and their suffering.

Immunohistochemistry

To prepare fixed brain tissue, the mice were anesthetized with sodium pentobarbital (50 mg/kg) and transcardially perfused with phosphate-buffered saline (PBS), followed by 4% paraformaldehyde (PFA) in 0.1 M phosphate buffer. The brains were placed in 4% PFA for 2 hours, followed by 30% sucrose in PBS. The brains were cut into 30-μm-thick coronal sections using a cryostat. The sections were rinsed before and between incubations with 0.1% Tween 20 (Sigma-Aldrich) in PBS (PBS-T). The sections were incubated for 1 hour in blocking solution (10% normal

goat serum in PBS-T) at room temperature and then incubated for 48 hours at 4°C with primary antibodies diluted in PBS-T. The following primary antibodies were used: guinea pig anti-CRH (1:800; Peninsula Laboratories), mouse anti-VGAT (1:500; Synaptic Systems), rabbit anti-$GABA_AR$ β2 (1:100; Novus Biologicals), guinea pig anti-NKCC1 [1 μg/ml; a gift from M. Watanabe, Hokkaido University School of Medicine; (*33*)], rabbit anti-KCC2 (1:500; Millipore), and rabbit anti-GFP for Venus and GCaMP3 (1:400; Molecular Probes). The following secondary antibodies were used: Alexa Fluor 488–conjugated goat anti–guinea pig; Alexa Fluor 488–conjugated goat anti-rabbit (1:200; Molecular Probes); and Alexa Fluor 594–conjugated goat anti-mouse, Alexa Fluor 594–conjugated goat anti-rabbit, and Alexa Fluor 594–conjugated goat anti–guinea pig (1:1000; Molecular Probes). The slides were mounted, and the cover-slipped sections were imaged using a confocal microscope (FV1000-D; Olympus) and a fluorescence microscope (BZ-9000; Keyence). For the assessments, we included three slides from one side of the PVN per mouse in which CRH immunohistochemistry was positive. The number, fluorescence intensity, and mean area of the CRH-immunoreactive cells were measured using ImageJ software [National Institutes of Health (NIH)].

Hormone analysis

The mice were euthanized via cervical dislocation, and the trunk blood was collected following decapitation and placed into polyethylene tubes with EDTA-2K (Becton, Dickinson and Company). Most samples were collected between 0900 and 1200 (light), whereas some samples were collected between 1900 and 2000 (dark). The samples were centrifuged at 3000 rpm for 20 min at 4°C, and the serum was collected and stored at −80°C until further use. To measure the CRH content, the hypothalamus was dissected out as previously reported (*59*). Briefly, following the removal of the brain from the decapitated mice, the hypothalamic blocks were dissected out on the basis of the following limits: the posterior border was the optic chiasm, the anterior border was the mammillary bodies, and the ventral border was the anterior cerebral commissure and the lateral hypothalamic nuclei. The hypothalamic blocks were immediately placed in cold (4°C), oxygenated, standard artificial cerebrospinal fluid (ACSF; 126.0 mM NaCl, 2.5 mM KCl, 1.25 mM NaH_2PO_4, 2.0 mM $MgSO_4$, 2.0 mM $CaCl_2$, 26.0 mM $NaHCO_3$, and 20.0 mM glucose). For sectioning, hypothalamic blocks were placed face up relative to the base of the brain in a vibratome (VT1000 S; Leica) and covered with ACSF; 500-μm coronal sections were collected to excise the ME, and 1000-μm coronal sections were collected to excise the PVN. We confirmed that the ME and the PVN of the $GAD67^{+/GFP}$ mice were clearly separated using a previously described method on the basis of fluorescence microscopy. The ME and PVN samples were homogenized via ultrasonic disruption in 500 μl of 1 N HCl, followed by centrifugation at 10,000 rpm for 15 min at 4°C, as previously reported (*60*). These aliquots were collected and stored at −80°C until further use. Plasma corticosterone, ACTH (*61*), and AVP levels (*62*) and hypothalamic CRH levels were determined using a RIA, as previously reported (*60*). Briefly, synthetic $[Tyr]_0$-$CRH_{1–41}$ was radioiodinated with $Na^{125}I$ using the chloramine T method. The labeled $[Tyr]_0$-$CRH_{1–41}$ samples were purified using a Sephadex G10 (Sigma-Aldrich) superfine column (1 cm × 5 cm) and further purified with a Sephadex G75 (Sigma-Aldrich) superfine column (1 cm × 20 cm). A 100-μl aliquot of each $CRH_{1–41}$ standard and sample was incubated with 100 μl of rabbit antiserum against $CRH_{1–41}$ (initial dilution, 1:15,000) at 4°C. The samples were assayed in duplicate. Following 1 day of incubation, 100 μl of labeled $[Tyr]_0$-$CRH_{1–41}$, which had been repurified using a Sephadex G50 (Sigma-Aldrich) superfine column (1 cm × 20 cm), was added, and the samples were incubated again for 1 day at 4°C. The antibody-bound and free peptides were separated via incubation with 100 μl of a secondary antibody (goat anti-rabbit γ-globulin) and 100 μl of 25% polyethylene glycol for 6 to 12 hours at 4°C, followed by centrifugation at 3000 rpm for 30 min at 4°C. The radioactivity bound to the antibody was counted in a γ-counter (ARC-7010; Aloka). The minimum detection limit of the assay was 2 pg per tube.

Restraint stress

The wild-type and $GAD67^{+/GFP}$ mice were physically restrained in a well-ventilated, 50-ml conical plastic tube for 30 min. Following restraint, the mice were euthanized, blood samples were collected, the mice were perfused with 4% PFA for fixation, and the brains were collected. Some wild-type mice received either 0.9% saline or bumetanide (30 mg/kg; Sigma-Aldrich) 15 min before the single 30-min bout of restraint-induced stress.

Surgery and microinfusion

A subgroup of mice underwent bilateral ADX or sham ADX. The ADX procedure was performed as previously described (*42*). All adrenalectomized mice were administered corticosterone (25 mg/liter; Tokyo Chemical Industry) in their drinking water for 5 days, followed by a 7-day recovery period. The mice were subsequently fixed with 4% PFA, and the fixed brain tissue was removed for CRH immunohistochemistry.

For microinfusions, the mice were anesthetized with sodium pentobarbital (50 mg/kg) and positioned in a stereotaxic apparatus, and their skulls were exposed. The mice subsequently received an intracerebroventricular injection of 2 μl of colchicine (7.5 mg in 1-ml 0.9% saline; Sigma-Aldrich). The target coordinates from bregma were 0.5 mm posterior, 1.0 mm lateral, and 2.0 mm ventral. Following the intracerebroventricular injection, the mice were housed in cages. Two days (48 hours) later, the mice were fixed with 4% PFA for subsequent CRH immunohistochemical analysis of the PVN.

In vivo application of muscimol

The effect of an intraperitoneal administration of the $GABA_AR$ agonist muscimol (2 mg/kg; Sigma-Aldrich) on the HPA axis was investigated. Muscimol was dissolved in 0.9% saline. In the control group, 0.9% saline without muscimol was administered via an intraperitoneal injection. Both muscimol and 0.9% saline were administered at a dose of 5 ml/kg. A blood sample and the brain tissue fixed following a 4% PFA infusion were collected 30 min after the injection for analysis via hormone titration and CRH immunohistochemistry, respectively.

Fluoro-Gold labeling

To label neurons that send monosynaptic projections to the ME, $GAD67^{+/GFP}$ mice received intraperitoneal injections of the retrogradely transportable marker compound Fluoro-Gold (40 mg/kg; Wako) (*21*). Four days after the injection, the brains were removed, and 100-μm-thick coronal brain sections were obtained using a vibrating microtome (Campden 7000smz-2; Campden Instruments Ltd.). Fluoro-Gold stainings in the PVN, SCN, DMH, VMH, and ARC were imaged under a fluorescence microscope using an excitation wavelength range of 340 to 380 nm, and emission was measured using a 610-nm long-pass filter.

Quantitative real-time PCR

The total RNA from the dissected hypothalamus was isolated with ISOGEN (Nippon Gene) according to the manufacturer's instructions. The

RNA was purified using RQ1 RNase-Free DNase (Promega) to eliminate genomic contamination, according to the manufacturer's instructions. The total RNA concentration was measured using a NanoDrop spectrophotometer. Complementary DNAs were subsequently synthesized from 0.5 μg of RNA per sample using SuperScript III Reverse Transcriptase (Invitrogen). Quantitative real-time PCR was performed on a Takara Thermal Cycler Dice (TP850) using primers and templates mixed with the SYBR Premix Ex Taq (Takara Bio Inc.). The primers for mouse CRH were as follows: forward, 5′-CCTGGGGAATCTCAACAGAA-3′; reverse, 5′-AACACGCGGAAAAAGTTAGC-3′ (120 base pairs) (*63*). The samples were amplified via an initial denaturation at 95°C for 30 s, followed by 40 cycles at 95°C for 5 s and 60°C for 30 s. The specificity of the reactions was determined via a dissociation curve analysis. The relative CRH mRNA levels were quantified using the comparative threshold cycle method for CRH mRNA and GAPDH, as previously reported (*64*).

Intracellular Ca^{2+} imaging

Brain sections (300 μm thick) were obtained from the CRH-GCaMP3 mice at postnatal days 21 to 25. Briefly, the brains were rapidly removed and placed in oxygenated, ice-cold, sucrose-modified ACSF (220 mM sucrose, 2.5 mM KCl, 1.25 mM NaH_2PO_4, 10.0 mM $MgSO_4$, 0.5 mM $CaCl_2$, 26.0 mM $NaHCO_3$, and 30.0 mM glucose). Coronal (PVN) or sagittal sections (ME) were obtained in the sucrose-modified ACSF using a vibratome, either VT1000 S (Leica) or Campden 7000smz-2 (Campden Instruments). The sections were subsequently maintained in oxygenated standard ACSF at room temperature before analysis. The sections were transferred to an imaging chamber that was perfused (2 ml/min) with oxygenated standard ACSF supplemented with 6-cyano-7-nitroquinoxaline-2,3-dione (10 μM; Tocris Bioscience) and D(−)-2-amino-5-phosphonopentanoic acid (50 μM; Tocris Bioscience) and maintained at 30°C. Confocal images were captured under a fluorescence microscope (BX51WI; Olympus) equipped with a spinning disc confocal unit (CSU-22; Yokogawa Electric) and an electron-multiplying CCD camera (iXon DV887; Andor). A 40× water immersion objective lens [0.8 numerical aperture (NA); Olympus] was mounted on a piezoelectric driver (Physik Instrumente) with its controller (Yokogawa Electric) to enable the rapid observation of the focal plane. The sections were excited with 488-nm wavelength light from a Sapphire 488-30 laser (Coherent Inc.) and visualized using band-pass emission filters [TXB538(2A); Asahi Glass]. Imaging was performed using iQ software (Andor). The cells or nerve terminals that exhibited GCaMP3 fluorescence were selected for analysis. Muscimol (10 μM; Sigma-Aldrich) was applied in the bath for 3.5 min after a 5-min control recording. Intracellular Ca^{2+} signals were collected every 5 s with *z*-axis increments of 4.5 μm at a depth of 67.5 to 75 μm from the first plane showing detectable fluorescence. The $\Delta F/F$ of each trial was calculated as $(F - F_0)/F_0$, where F_0 is the baseline fluorescence signal averaged over a 25-s period immediately before the start of the application of muscimol. At the end of each imaging session, the viability of the section was confirmed via the application of 50 mM K^+ (72.0 mM NaCl, 50.0 mM KCl, 1.0 mM KH_2PO_4, 1.0 mM $MgCl_2$, 2.0 mM $CaCl_2$, 26.0 mM $NaHCO_3$, and 10.0 mM glucose), and only the sections that responded to high K^+ were included in the analysis. The data were analyzed using AquaCosmos software (Hamamatsu Photonics).

Fluorescence images of GCaMP3 were also acquired using a two-photon microscope (LSM-7MP; Carl Zeiss) equipped with a water immersion objective lens (W Plan-Apochromat 20×; NA, 1.0) and a Ti:Sapphire laser (Chameleon Vision II, Coherent Inc.) emitting at 920 nm, together with a 500- to 550-nm band-pass optical filter. Bumetanide (10 μM) was applied to the bath starting at least 15 min before the recordings and was continuously perfused during the recordings. Three ROIs on the GCaMP3-positive terminals were randomly selected from each terminal cluster for quantitative analysis. The data were analyzed using NIH ImageJ software and Imaris 7.2.2 (Bitplane).

Statistical analyses

All statistical analyses were performed using IBM SPSS Statistics software (version 21). For comparisons of two data sets, statistical significance was determined using Student's *t* tests. All results are expressed as means ± SEM. Differences were considered significant at $P < 0.05$.

SUPPLEMENTARY MATERIALS

Supplementary material for this article is available at http://advances.sciencemag.org/cgi/content/full/2/8/e1501723/DC1

fig. S1. CRH immunohistochemistry in the homozygous CRH-iCre embryos.

fig. S2. Muscimol administration in the wild-type mice.

fig. S3. NKCC1 and KCC2 expression patterns in the CRH neurons of the PVN and ME following acute stress.

fig. S4. Summary diagram of PVN-ARC-ME triangle interconnected by GABAergic neurons, indicating the differential GABAergic actions on CRH neurons at the PVN and ME in relation to changes in Cl^- homeostasis.

REFERENCES AND NOTES

1. M. Palkovits, Neuropeptides in the hypothalamo-hypophyseal system: Lateral retrochiasmatic area as a common gate for neuronal fibers towards the median eminence. *Peptides* **5**, 35–39 (1984).
2. Z. Liposits, T. Görcs, G. Sétáló, I. Lengvári, B. Flerkó, S. Vigh, A. V. Schally, Ultrastructural characteristics of immunolabelled, corticotropin releasing factor (CRF)-synthesizing neurons in the rat brain. *Cell Tissue Res.* **229**, 191–196 (1983).
3. B. H. Levy, J. G. Tasker, Synaptic regulation of the hypothalamic–pituitary–adrenal axis and its modulation by glucocorticoids and stress. *Front. Cell. Neurosci.* **6**, 1–13 (2012).
4. M. G. Erlander, N. J. K. Tillakaratne, S. Feldblum, N. Patel, A. J. Tobin, Two genes encode distinct glutamate decarboxylases. *Neuron* **7**, 91–100 (1991).
5. B. L. Roland, P. E. Sawchenko, Local origins of some GABAergic projections to the paraventricular and supraoptic nuclei of the hypothalamus in the rat. *J. Comp. Neurol.* **332**, 123–143 (1993).
6. J. G. Tasker, F. E. Dudek, Local inhibitory synaptic inputs to neurones of the paraventricular nucleus in slices of rat hypothalamus. *J. Physiol.* **469**, 179–192 (1993).
7. G. Bowers, W. E. Cullinan, J. P. Herman, Region-specific regulation of glutamic acid decarboxylase (GAD) mRNA expression in central stress circuits. *J. Neurosci.* **18**, 5938–5947 (1998).
8. J. G. Tasker, C. Boudaba, L. A. Schrader, Local glutamatergic and GABAergic synaptic circuits and metabotropic glutamate receptors in the hypothalamic paraventricular and supraoptic nuclei. *Adv. Exp. Med. Biol.* **449**, 117–121 (1998).
9. J. J. Radley, K. L. Gosselink, P. E. Sawchenko, A discrete GABAergic relay mediates medial prefrontal cortical inhibition of the neuroendocrine stress response. *J. Neurosci.* **29**, 7330–7340 (2009).
10. C. Rivera, J. Voipio, J. A. Payne, E. Ruusuvuori, H. Lahtinen, K. Lamsa, U. Pirvola, M. Saarma, K. Kaila, The K^+/Cl^- co-transporter KCC2 renders GABA hyperpolarizing during neuronal maturation. *Nature* **397**, 251–255 (1999).
11. S. A. Hewitt, J. I. Wamsteeker, E. U. Kurz, J. S. Bains, Altered chloride homeostasis removes synaptic inhibitory constraint of the stress axis. *Nat. Neurosci.* **12**, 438–443 (2009).
12. J. Sarkar, S. Wakefield, G. MacKenzie, S. J. Moss, J. Maguire, Neurosteroidogenesis is required for the physiological response to stress: Role of neurosteroid-sensitive $GABA_A$ receptors. *J. Neurosci.* **31**, 18198–18210 (2011).
13. S. Miller, J. Maguire, Deficits in KCC2 and activation of the HPA axis lead to depression-like behavior following social defeat. *Horm. Stud.* **2**, 2 (2014).
14. N. Tamamaki, Y. Yanagawa, R. Tomioka, J.-I. Miyazaki, K. Obata, T. Kaneko, Green fluorescent protein expression and colocalization with calretinin, parvalbumin, and somatostatin in the GAD67-GFP knock-in mouse. *J. Comp. Neurol.* **467**, 60–79 (2003).

15. T. Uchida, Y. Oki, Y. Yanagawa, A. Fukuda, A heterozygous deletion in the glutamate decarboxylase 67 gene enhances maternal and fetal stress vulnerability. *Neurosci. Res.* **69**, 276–282 (2011).
16. S. R. Vincent, T. Hökfelt, J.-Y. Wu, GABA neuron systems in hypothalamus and the pituitary gland. Immunohistochemical demonstration using antibodies against glutamate decarboxylase. *Neuroendocrinology* **34**, 117–125 (1982).
17. S. Pirker, C. Schwarzer, A. Wieselthaler, W. Sieghart, G. Sperk, $GABA_A$ receptors: Immunocytochemical distribution of 13 subunits in the adult rat brain. *Neuroscience* **101**, 815–850 (2000).
18. G. E. Gillies, E. A. Linton, P. J. Lowry, Corticotropin releasing activity of the new CRF is potentiated several times by vasopressin. *Nature* **299**, 355–357 (1982).
19. M. L. Tappaz, W. H. Oertel, M. Wassef, E. Mugnaini, Central GABAergic neuroendocrine regulations: Pharmacological and morphological evidence. *Prog. Brain Res.* **55**, 77–96 (1982).
20. C. Acuna-Goycolea, N. Tamamaki, Y. Yanagawa, K. Obata, A. N. van den Pol, Mechanisms of neuropeptide Y, peptide YY, and pancreatic polypeptide inhibition of identified green fluorescent protein-expressing GABA neurons in the hypothalamic neuroendocrine arcuate nucleus. *J. Neurosci.* **25**, 7406–7419 (2005).
21. L. Ozcan, A. S. Ergin, A. Lu, J. Chung, S. Sarkar, D. Nie, M. G. Myers Jr., U. Ozcan, Endoplasmic reticulum stress plays a central role in development of leptin resistance. *Cell Metab.* **9**, 35–51 (2009).
22. K. Egawa, A. Fukuda, Pathophysiological power of improper tonic $GABA_A$ conductances in mature and immature models. *Front. Neural Circuits* **7**, 170 (2013).
23. W. Kilb, S. Kirischuk, H. J. Luhmann, Role of tonic GABAergic currents during pre- and early postnatal rodent development. *Front. Neural Circuits* **7**, 139 (2013).
24. V. Lee, J. Sarkar, J. Maguire, Loss of *Gabrd* in CRH neurons blunts the corticosterone response to stress and diminishes stress-related behaviors. *Psychoneuroendocrinology* **41**, 75–88 (2014).
25. Y. Ben-Ari, Excitatory actions of GABA during development: The nature of the nurture. *Nat. Rev. Neurosci.* **3**, 728–739 (2002).
26. J. Yamada, A. Okabe, H. Toyoda, W. Kilb, H. J. Luhmann, A. Fukuda, Cl^- uptake promoting depolarizing GABA actions in immature rat neocortical neurones is mediated by NKCC1. *J. Physiol.* **557**, 829–841 (2004).
27. I. S. Jang, H. J. Jeong, N. Akaike, Contribution of the Na-K-Cl cotransporter on $GABA_A$ receptor-mediated presynaptic depolarization in excitatory nerve terminals. *J. Neurosci.* **21**, 5962–5972 (2001).
28. I.-S. Jang, M. Nakamura, Y. Ito, N. Akaike, Presynaptic $GABA_A$ receptors facilitate spontaneous glutamate release from presynaptic terminals on mechanically dissociated rat CA3 pyramidal neurons. *Neuroscience* **138**, 25–35 (2006).
29. C. Wang, K. Ohno, T. Furukawa, T. Ueki, M. Ikeda, A. Fukuda, K. Sato, Differential expression of KCC2 accounts for the differential GABA responses between relay and intrinsic neurons in the early postnatal rat olfactory bulb. *Eur. J. Neurosci.* **21**, 1449–1455 (2005).
30. R. Turecek, L. O. Trussell, Presynaptic glycine receptors enhance transmitter release at a mammalian central synapse. *Nature* **411**, 587–590 (2001).
31. S. J. Zhang, M. B. Jackson, GABAA receptor activation and the excitability of nerve terminals in the rat posterior pituitary. *J. Physiol.* **483**, 583–595 (1995).
32. G. D. Price, L. O. Trussell, Estimate of the chloride concentration in a central glutamatergic terminal: A gramicidin perforated-patch study on the calyx of Held. *J. Neurosci.* **26**, 11432–11436 (2006).
33. B. Wei, T. Kumada, T. Furukawa, K. Inoue, M. Watanabe, K. Sato, A. Fukuda, Pre- and postsynaptic switches of GABA actions associated with Cl^- homeostatic changes are induced in the spinal nucleus of the trigeminal nerve in a rat model of trigeminal neuropathic pain. *Neuroscience* **228**, 334–348 (2013).
34. F. J. Alvarez-Leefmans, M. León-Olea, J. Mendoza-Sotelo, F. J. Alvarez, B. Antón, R. Garduño, Immunolocalization of the Na^+–K^+–$2Cl^-$ cotransporter in peripheral nervous tissue of vertebrates. *Neuroscience* **104**, 569–582 (2001).
35. S. J. Zhang, M. B. Jackson, GABA-activated chloride channels in secretory nerve endings. *Science* **259**, 531–534 (1993).
36. B. Graham, S. Redman, A simulation of action potentials in synaptic boutons during presynaptic inhibition. *J. Neurophysiol.* **71**, 538–549 (1994).
37. D. Cattaert, A. El Marina, Shunting versus inactivation: Analysis of presynaptic inhibitory mechanisms in primary afferents of the crayfish. *J. Neurosci.* **19**, 6079–6089 (1999).
38. P. Rudomin, R. F. Schmidt, Presynaptic inhibition in the vertebrate spinal cord revisited. *Exp. Brain Res.* **129**, 1–37 (1999).
39. G. B. Awatramani, G. D. Price, L. O. Trussell, Modulation of transmitter release by presynaptic resting potential and background calcium levels. *Neuron* **48**, 109–121 (2005).
40. K. Achilles, A. Okabe, M. Ikeda, C. Shimizu-Okabe, J. Yamada, A. Fukuda, H. J. Luhmann, W. Kilb, Kinetic properties of Cl^- uptake mediated by Na^+-dependent K^+-$2Cl^-$ cotransport in immature rat neocortical neurons. *J. Neurosci.* **27**, 8616–8627 (2007).
41. Y. Chen, J. Molet, B. G. Gunn, K. Ressler, T. Z. Baram, Diversity of reporter expression patterns in transgenic mouse lines targeting corticotropin-releasing hormone-expressing neurons. *Endocrinology* **156**, 4769–4780 (2015).
42. K. Itoi, A. H. Talukder, T. Fuse, T. Kaneko, R. Ozawa, T. Sato, T. Sugaya, K. Uchida, M. Yamazaki, M. Abe, R. Natsume, K. Sakimura, Visualization of corticotropin-releasing factor neurons by fluorescent proteins in the mouse brain and characterization of labeled neurons in the paraventricular nucleus of the hypothalamus. *Endocrinology* **155**, 4054–4060 (2014).
43. B. S. McEwen, Physiology and neurobiology of stress and adaptation: Central role of the brain. *Physiol. Rev.* **87**, 873–904 (2007).
44. R. M. Sapolsky, Why stress is bad for your brain. *Science* **273**, 749–750 (1996).
45. M. W. Schwartz, S. C. Woods, D. Porte Jr., R. J. Seeley, D. G. Baskin, Central nervous system control of food intake. *Nature* **404**, 661–671 (2000).
46. Y. Uehara, H. Shimizu, K. Ohtani, N. Sato, M. Mori, Hypothalamic corticotropin-releasing hormone is a mediator of the anorexigenic effect of leptin. *Diabetes* **47**, 890–893 (1998).
47. K. T. Kahle, T. Z. Deeb, M. Puskarjov, L. Silayeva, B. Liang, K. Kaila, S. J. Moss, Modulation of neuronal activity by phosphorylation of the K–Cl cotransporter KCC2. *Trends Neurosci.* **36**, 726–737 (2013).
48. D. R. Alessi, J. Zhang, A. Khanna, T. Hochdörfer, Y. Shang, K. T. Kahle, The WNK-SPAK/OSR1 pathway: Master regulator of cation-chloride cotransporters. *Sci. Signal.* **7**, re3 (2014).
49. D. Arion, D. A. Lewis, Altered expression of regulators of the cortical chloride transporters NKCC1 and KCC2 in schizophrenia. *Arch. Gen. Psychiatry* **68**, 21–31 (2011).
50. V. Di Marzo, I. Matias, Endocannabinoid control of food intake and energy balance. *Nat. Neurosci.* **8**, 585–589 (2005).
51. C. Cansell, R. G. P. Denis, A. Joly-Amado, J. Castel, S. Luquet, Arcuate AgRP neurons and the regulation of energy balance. *Front. Endocrinol.* **3**, 1–7 (2012).
52. D. Kong, Q. Tong, C. Ye, S. Koda, P. M. Fuller, M. J. Krashes, L. Vong, R. S. Ray, D. P. Olson, B. B. Lowell, GABAergic RIP-Cre neurons in the arcuate nucleus selectively regulate energy expenditure. *Cell* **151**, 645–657 (2012).
53. Y. Ben-Ari, M. A. Woodin, E. Sernagor, L. Cancedda, L. Vinay, C. Rivera, P. Legendre, H. J. Luhmann, A. Bordey, P. Wenner, A. Fukuda, A. N. van den Pol, J.-L. Gaiarsa, E. Cherubini, Refuting the challenges of the developmental shift of polarity of GABA actions: GABA more exciting than ever! *Front. Cell. Neurosci.* **6**, 35 (2012).
54. M. K. Herde, K. J. Iremonger, S. Constantin, A. E. Herbison, GnRH neurons elaborate a long-range projection with shared axonal and dendritic functions. *J. Neurosci.* **33**, 12689–12697 (2013).
55. M. Watanabe, A. Fukuda, J. Nabekura, The role of GABA in the regulation of GnRH neurons. *Front. Neurosci.* **8**, 387 (2014).
56. K. Berglund, W. Schleich, H. Wang, G. Feng, W. C. Hall, T. Kuner, G. J. Augustine, Imaging synaptic inhibition throughout the brain via genetically targeted Clomeleon. *Brain Cell Biol.* **36**, 101–118 (2008).
57. L. Batti, M. Mukhtarov, E. Audero, A. Ivanov, R. C. Paolicelli, S. Zurborg, C. Gross, P. Bregestovski, P. A. Heppenstall, Transgenic mouse lines for non-invasive ratiometric monitoring of intracellular chloride. *Front. Mol. Neurosci.* **6**, 11 (2013).
58. H. A. Zariwala, B. G. Borghuis, T. M. Hoogland, L. Madisen, L. Tian, C. I. De Zeeuw, H. Zeng, L. L. Looger, K. Svoboda, T.-W. Chen, A Cre-dependent GCaMP3 reporter mouse for neuronal imaging in vivo. *J. Neurosci.* **32**, 3131–3141 (2012).
59. S. Tsagarakis, J. M. P. Holly, L. H. Rees, G. M. Besser, A. Grossman, Acetylcholine and norepinephrine stimulate the release of corticotropin-releasing factor-41 from the rat hypothalamus in vitro. *Endocrinology* **123**, 1962–1969 (1988).
60. P. B. Chappell, M. A. Smith, C. D. Kilts, G. Bissette, J. Ritchie, C. Anderson, C. B. Nemeroff, Alterations in corticotropin-releasing factor-like immunoreactivity in discrete rat brain regions after acute and chronic stress. *J. Neurosci.* **6**, 2908–2914 (1986).
61. K. Yogo, Y. Oki, K. Iino, M. Yamashita, S. Shibata, C. Hayashi, S. Sasaki, T. Suenaga, D. Nakahara, H. Nakamura, Neuropeptide W stimulates adrenocorticotrophic hormone release via corticotrophin-releasing factor but not via arginine vasopressin. *Endocr. J.* **59**, 547–554 (2012).
62. Y. Oki, S. Ohgo, T. Yoshimi, A sensitive and specific radioimmunoassay for arginine vasopressin and its validation. *Nihon Naibunpi Gakkai Zasshi* **60**, 183–194 (1984).
63. M. Simard, M. Côté, P. R. Provost, Y. Tremblay, Expression of genes related to the hypothalamic-pituitary-adrenal axis in murine fetal lungs in late gestation. *Reprod. Biol. Endocrinol.* **8**, 134 (2010).
64. K. J. Livak,T. D. Schmittgen, Analysis of relative gene expression data using real-time quantitative PCR and the $2^{-\Delta\Delta C_T}$ method. *Methods* **25**, 402–408 (2001).

Acknowledgments: We are grateful to M. Watanabe (Hokkaido University School of Medicine) for the gift of the anti-NKCC1 antibody. **Funding:** This work was supported by Grants-in-Aid for Scientific Research on Innovative Areas (nos. 26110705 and 15H05872) from the Ministry of Education, Culture, Sports, Science, and Technology of Japan (to A.F.); Grants-in-Aid for Scientific Research (B) (no. 25293052) and for Challenging Exploratory Research (no. 26670512) from the Japan Society for the Promotion of Science (to A.F.); and a grant for a Practical Research Project for Rare/Intractable Diseases (no. 27280301) from the Japan Agency for Medical Research and

Development. **Author contributions:** K.K., M.W., Y.O., and A.F. conceived the study. K.K. performed the experiments with the assistance of H.M. for the two-photon imaging. Y.Y. and K.I. generated the genetically modified mice. Y.O., M.Y., Y.Y., K.I., T.S., and A.F. contributed to the supervision and interpretation of the experiments. K.K. and A.F. wrote the manuscript. **Competing interests:** The authors declare that they have no competing interests. **Data and materials availability:** All data needed to evaluate the conclusions in the paper are present in the paper and/or the Supplementary Materials. Additional data related to this paper may be requested from the authors.

Submitted 28 November 2015
Accepted 19 July 2016
Published 17 August 2016
10.1126/sciadv.1501723

Citation: K. Kakizawa, M. Watanabe, H. Mutoh, Y. Okawa, M. Yamashita, Y. Yanagawa, K. Itoi, T. Suda, Y. Oki, A. Fukuda, A novel GABA-mediated corticotropin-releasing hormone secretory mechanism in the median eminence. *Sci. Adv.* **2**, e1501723 (2016).

ScienceAdvances
AAAS

A novel GABA-mediated corticotropin-releasing hormone secretory mechanism in the median eminence

Keisuke Kakizawa, Miho Watanabe, Hiroki Mutoh, Yuta Okawa, Miho Yamashita, Yuchio Yanagawa, Keiichi Itoi, Takafumi Suda, Yutaka Oki and Atsuo Fukuda (August 17, 2016)
Sci Adv 2016, 2:.
doi: 10.1126/sciadv.1501723